

Rare Example of μ -Nitrito- $1\kappa^2O, O':2\kappa O$ Coordinating Mode in Copper(II) Nitrite Complexes with Monoanionic Tridentate Schiff Base Ligands: Structure, Magnetic, and Electrochemical Properties

Biswarup Sarkar,^{†,‡} Sanjit Konar,[§] Carlos J. Gómez-García,^{*,||} and Ashutosh Ghosh^{*,†}

Department of Chemistry, University College of Science, University of Calcutta, 92, APC Road, Kolkata-700 009, India, Bolpur College, Bolpur, West Bengal, PIN-731204, India, Fakultät für Chemie, Universität Bielefeld, D33615, Bielefeld, Germany, and Instituto de Ciencia Molecular (ICMol), Parque Científico, Universidad de Valencia, 46980 Paterna, Valencia, Spain

Received June 23, 2008

Three new copper(II) complexes, $[\text{CuL}^1(\text{NO}_2)]_n$ (**1**), $[\text{CuL}^2(\text{NO}_2)]$ (**2**), and $[\text{CuL}^3(\text{NO}_2)]$ (**3**), with three similar tridentate Schiff base ligands [$\text{HL}^1 = 6\text{-amino-3-methyl-1-phenyl-4-azahept-2-en-1-one}$, $\text{HL}^2 = 6\text{-amino-3-methyl-1-phenyl-4-azahex-2-en-1-one}$, and $\text{HL}^3 = 6\text{-diethylamino-3-methyl-1-phenyl-4-azahex-2-en-1-one}$] have been synthesized and characterized structurally and magnetically. In all three complexes, the tridentate Schiff base ligand and one oxygen atom of the nitrite ion constitute the equatorial plane around Cu(II), whereas the second oxygen atom of the nitrite ligand coordinates to one of the axial positions. In **1**, this axially coordinated oxygen atom of the nitrite ligand also coordinates weakly to the other axial position of a Cu(II) ion of another unit to form a one-dimensional chain with the μ -nitrito- $1\kappa^2O, O':2\kappa O$ bridging mode. Complexes **2** and **3** are discrete monomers that are joined together by intermolecular H bonds and $\text{C-H}\cdots\pi$ interactions in **2** and by only $\text{C-H}\cdots\pi$ interactions in **3**. A weak antiferromagnetism ($J = -1.96(2) \text{ cm}^{-1}$) is observed in complex **1** due to its asymmetric nitrite bridging. Complexes **2** and **3** show very weak antiferromagnetic interactions ($J = -0.089$ and -0.096 cm^{-1} , respectively) attributed to the presence of intermolecular H-bonding and $\text{C-H}\cdots\pi$ interactions. The corresponding Cu(I) species produced by the electrochemical reduction of complexes **1** and **2** disproportionate to Cu^0 and Cu^{2+} , whereas the reduced Cu(I) species of complex **3** seems to be stable presumably due to a higher tetrahedral distortion of the equatorial plane in **3** compared to that in **1** and **2**.

Introduction

Copper(II) nitrite complexes have been of interest for a long time, mainly in connection with the reaction mechanism of copper-containing nitrite reductases.¹ Recently, there has

been an increasing interest in nitrite-bridged polynuclear complexes associated with the study of the sign and strength of the magnetic interactions mediated by their different bridging modes.² The NO_2 group coordinates to the metal atom as a nitro (via the nitrogen), a nitrito (via an oxygen), and a chelating ligand (via both oxygen atoms) to yield mononuclear complexes. On the other hand, five bridging modes (Scheme 1) of the nitrite ion have been identified in polynuclear compounds.^{2b}

The two-atom O/N-bridging mode (Scheme 1a) is the most common one, and it usually shows moderate antiferromagnetic interactions.³ The tridentate bridging modes in which the NO_2^- ion is chelated to one metal through the two

* Author to whom correspondence should be addressed. E-mail: ghosh_59@yahoo.com (A.G.), carlos.gomez@uv.es (C.J.G.G.).

[†] University of Calcutta.

[‡] Bolpur College.

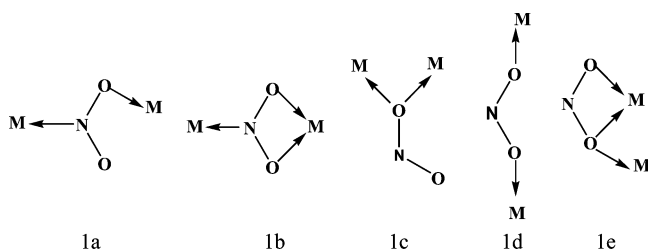
[§] Universität Bielefeld.

^{||} Universidad de Valencia.

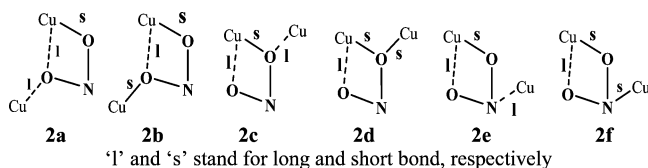
(1) (a) George, G. N.; Mertens, J. A.; Campbell, W. H. *J. Am. Chem. Soc.* **1999**, *121*, 9730. (b) Kroneck, P. M. H.; Beuerle, J.; Schumacher, W. *Degradation of Environmental Pollutants by Microorganisms and their Metalloenzymes*; Sigel, H., Sigel, A., Eds.; Marcel Dekker: New York, 1992; Vol. 28, pp 455–505. (c) Adman, E. T.; Turley, S. K. *Bioinorganic Chemistry of Copper*; Karlin, K. D., Tyekla'r, Z., Eds.; Chapman & Hall, Inc.: New York, 1993; pp 397–405. (d) Godden, J. W.; Turley, S.; Teller, K. C. *Science* **1991**, *253*, 438. (e) Tolman, W. B. *J. Biol. Inorg. Chem.* **2006**, *11*, 261, and references therein.

(2) (a) Hitchman, M. A.; Rowbottom, C. *Coord. Chem. Rev.* **1982**, *42*, 55. (b) Liu, T.; Chen, Y. H.; Zhang, Y. J.; Wang, Z. M.; Gao, S. *Inorg. Chem.* **2006**, *45*, 9148, and references therein.

Scheme 1



Scheme 2

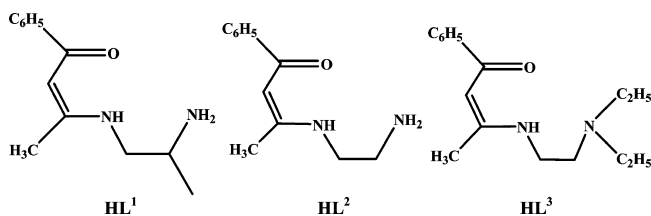


oxygens and bridged to a second metal ion either through the nitrogen atom (Scheme 1b) or through one of the chelating oxygen atoms (Scheme 1e) are relatively uncommon. In copper(II), such modes can occur in even more versatile ways,⁴ as the axial and equatorial bonds are distinguishable (Scheme 2). Variable-temperature magnetic studies of a few complexes having such tridentate bridging modes of nitrite have been reported.^{4a,b,5} However, in most cases, the presence of another bridging group, which mediates magnetic exchange more efficiently, makes the assignment of coupling constants through such nitrite bridges very difficult.^{4,5} To our knowledge, there is only one report of a copper(II) complex in which the copper centers are bridged by no other groups than the tridentate bridging nitrite (Scheme 2c), and the coligand in that complex is a tridentate N,N,O donor Schiff base.⁶ A weak ferromagnetic interaction is found in that dinuclear complex.⁶

In this paper, we report the synthesis and crystal structure of three Cu(II) nitrite complexes with the general formula $\text{Cu}(\text{L}^n)(\text{NO}_2)$, where HL^n ($n = 1-3$) are three tridentate Schiff bases derived from three different diamines and 1-benzoylacetone (Scheme 3: $\text{HL}^1 = [6\text{-amino-3-methyl-1-phenyl-4-azahept-2-en-1-one}]$, $\text{HL}^2 = [6\text{-amino-3-methyl-1-phenyl-4-azahex-2-en-1-one}]$, and $\text{HL}^3 = [6\text{-diethylamino-3-methyl-1-phenyl-4-azahex-2-en-1-one}]$).

Complex $[\text{Cu}(\text{L}^1)(\text{NO}_2)]_n$ (**1**) is a polymeric chain compound with tridentate $\mu\text{-nitrito-1}\kappa^2\text{O},\text{O}':2\kappa\text{O}$ bridging mode (Scheme 2a). This mode has been found previously only in

Scheme 3



one compound, but along with other bridging modes of the nitrite ion and the coupling through this bridge remains unexplored.^{4b} As compound **1** does not contain any other bridge between the copper(II), provides the first opportunity to study the magnetic coupling through this bridge. Complexes $[\text{Cu}(\text{L}^2)(\text{NO}_2)]$ (**2**) and $[\text{Cu}(\text{L}^3)(\text{NO}_2)]$ (**3**) are discrete mononuclear species, with intermolecular H-bonding and $\text{C-H}\cdots\pi$ interactions occurring in **2** and only $\text{C-H}\cdots\pi$ interactions in **3**. The variable-temperature magnetic properties of **1-3** are also reported here.

Experimental Section

The diamines and 1-benzoylacetone were purchased from Lancaster and were of reagent grade. They were used as received without further purification. The three monocondensed ligands HL^1 , HL^2 , and HL^3 (Scheme 3) have been synthesized in our laboratory according to methods described earlier.^{7,8}

Synthesis of Complexes $[\text{Cu}(\text{L}^1)(\text{NO}_2)]_n$ (1**), $[\text{Cu}(\text{L}^2)(\text{NO}_2)]$ (**2**), and $[\text{Cu}(\text{L}^3)(\text{NO}_2)]$ (**3**).** A solution of $\text{Cu}(\text{CH}_3\text{COO})_2\cdot\text{H}_2\text{O}$ (1.99 g, 10 mmol) in methanol (20 mL) was added to a stirred solution of each of the ligands, HL^1 , HL^2 , and HL^3 (10 mmol), in methanol (10 mL). Triethylamine (1.7 mL, 10 mmol) was then added dropwise to this solution with constant stirring. The resulting solution was filtered to remove a small amount of colloidal precipitate that was formed immediately after the addition of triethylamine. Sodium nitrite (0.69 g, 10 mmol) dissolved in methanol (10 mL) was added to this solution with constant stirring. Microcrystalline greenish-blue products formed for all three compounds upon keeping the filtrate overnight at room temperature. They were filtered and recrystallized from dry methanol. Single crystals of the compounds were obtained by slow evaporation of the methanol solution in a refrigerator.

Complex 1. Yield: 1.9 g (57%). Anal. calcd for $\text{C}_{13}\text{H}_{17}\text{CuN}_3\text{O}_3$: C, 47.77; H, 5.24; N, 12.86. Found: C, 47.94; H, 5.22; N, 12.71%. $\lambda_{\text{max}}/\text{nm}$ ($\epsilon_{\text{max}}/\text{dm}^3 \text{ mol}^{-1} \text{ cm}^{-1}$) (methanol): 610 (218), 377 (440), 279 (529), 247 (1128). IR: $\nu(\text{C}=\text{N})$, 1517 cm^{-1} ; $\nu(\text{N}-\text{H})$, 3229 and 3306 cm^{-1} ; $\nu_s(\text{NO}_2)$, 1337 cm^{-1} ; $\nu_{\text{as}}(\text{NO}_2)$, 1169 cm^{-1} ; $\delta(\text{NO}_2)$, 837 cm^{-1} .

Complex 2. Yield: 2.1 g (68%). Anal. calcd for $\text{C}_{12}\text{H}_{15}\text{CuN}_3\text{O}_3$: C, 46.08; H, 4.83; N, 13.43. Found: C, 46.32; H, 4.96; N, 13.57%. $\lambda_{\text{max}}/\text{nm}$ ($\epsilon_{\text{max}}/\text{dm}^3 \text{ mol}^{-1} \text{ cm}^{-1}$) (methanol): 608 (187), 376 (504),

- (3) (a) Meyer, A.; Gleizers, A.; Girerd, J. J.; Verdager, M.; Kahn, O. *Inorg. Chem.* **1982**, *21*, 1729. (b) Escuer, A.; Vicente, R.; Solans, X. *J. Chem. Soc., Dalton Trans.* **1997**, 531. (c) Rajendiran, T. M.; Kahn, O.; Golhen, S.; Ouahab, L.; Honda, Z.; Katsumata, K. *Inorg. Chem.* **1998**, *37*, 5693. (d) McKee, C.; Zvagulis, M.; Reed, C. A. *Inorg. Chem.* **1985**, *24*, 2914. (e) Blake, A. J.; Hill, S. J.; Hubberstey, P. *Chem. Commun.* **1998**, 1587. (f) Tolman, W. B. *Inorg. Chem.* **1991**, *30*, 4877. (g) Begley, M. J.; Hubberstey, P.; Stroud, J. *J. Chem. Soc., Dalton Trans.* **1996**, 4295.
- (4) (a) Costes, J. P.; Dahan, F.; Laurent, J. P.; Drillon, M. *Inorg. Chim. Acta* **1999**, *294*, 8. (b) Escuer, A.; El Fallah, M. S.; Vicente, R.; Sanz, N.; Font-Bardia, M.; Solans, X.; Mautner, F. A. *Dalton Trans* **2004**, 1867. (c) Halfen, J. A.; Mahapatra, S.; Olmstead, M. M.; Tolman, W. B. *J. Am. Chem. Soc.* **1994**, *116*, 2173.
- (5) Diaz, C.; Ribas, J.; Costa, R.; Tercero, J.; El Fallah, M. S.; Solans, X.; Font-Bardia, M. *Eur. J. Inorg. Chem.* **2000**, 675.
- (6) Costes, J. P.; Dahan, F.; Ruiz, J.; Laurent, J. P. *Inorg. Chim. Acta* **1995**, *239*, 53.

- (7) (a) Costes, J. P.; Dahan, F.; Laurent, J. P. *Inorg. Chem.* **1986**, *25*, 413. (b) Kwiatkowski, M.; Kwiatkowski, E.; Olechnowicz, A.; Ho, D. M.; Deutsch, E. *Inorg. Chim. Acta* **1988**, *150*, 65. (c) Ray, M. S.; Chattopadhyay, S.; Drew, M. G. B.; Figuerola, A.; Ribas, J.; Diaz, C.; Ghosh, A. *Eur. J. Inorg. Chem.* **2005**, 4562. (d) Sarkar, B.; Ray, M. S.; Drew, M. G. B.; Figuerola, A.; Diaz, C.; Ghosh, A. *Polyhedron* **2006**, *25*, 3084, and references therein.
- (8) (a) Sarkar, B.; Ray, M. S.; Drew, M. G. B.; Lu, C. Z.; Ghosh, A. *J. Coord. Chem.* **2007**, *60*, 2165. (b) Sarkar, B.; Bocelli, G.; Cantoni, A.; Ghosh, A. *J. Coord. Chem.* DOI: 10.1080/00958970802216685; published online July 30, 2008. (c) Sarkar, B.; Drew, M. G. B.; Estrader, M.; Diaz, C.; Ghosh, A. *Polyhedron* **2008**, *27*, 2625.

Table 1. Crystal Data and Structure Refinement of Complexes 1–3

compound	1	2	3
formula	C ₁₃ H ₁₇ CuN ₃ O ₃	C ₁₂ H ₁₅ CuN ₃ O ₃	C ₁₆ H ₂₃ CuN ₃ O ₃
<i>M</i>	326.84	312.54	368.91
crystal system	monoclinic	orthorhombic	monoclinic
space group	<i>P</i> 2 ₁ / <i>n</i>	<i>Pbca</i>	<i>P</i> 2 ₁ / <i>c</i>
<i>a</i> /Å	11.14(1)	7.23(1)	7.83 (1)
<i>b</i> /Å	8.14(1)	13.30(1)	16.04(1)
<i>c</i> /Å	16.06(1)	26.51(1)	13.00(1)
β /deg	108.62(1)	90	90.51(1)
<i>V</i> /Å ³	1381.1(3)	2550(2)	1633.5(4)
<i>Z</i>	4	8	4
<i>D</i> _c /g cm ⁻³	1.572	1.630	1.500
μ /mm ⁻¹	1.6[Mo K α]	1.7[Mo K α]	1.4[Mo K α]
<i>R</i> (int)	0.028	0.046	0.023
no. of unique data	3086	2140	3669
no. of data with <i>I</i> > 2 σ (<i>I</i>)	2817	2008	3220
<i>R</i> 1, <i>wR</i> 2	0.0437, 0.1201	0.0268, 0.0926	0.0459, 0.1222
goodness-of-fit on <i>F</i> ²	1.119	1.192	1.101

278 (478), 243 (1104). IR: ν (C=N), 1508 cm⁻¹; ν (N–H), 3258 and 3306 cm⁻¹; ν_s (NO₂), 1370 cm⁻¹; ν_{as} (NO₂), 1069 cm⁻¹; δ (NO₂), 828 cm⁻¹.

Complex 3. Yield: 2.0 g (55%). Anal. calcd for C₁₆H₂₃CuN₃O₃: C, 52.09; H, 6.28; N, 11.39. Found: C, 51.96; H, 6.31; N, 11.43%. λ_{max}/nm ($\epsilon_{max}/dm^3 mol^{-1} cm^{-1}$) (methanol): 587 (181), 374(448), 286 (465), 246 (1089). IR: ν (C=N), 1508 cm⁻¹; ν_s (NO₂), 1365 cm⁻¹; ν_{as} (NO₂), 1029 cm⁻¹; δ (NO₂), 830 cm⁻¹.

Physical Measurements. Elemental analyses (carbon, hydrogen, and nitrogen) were performed using a Perkin-Elmer 240C elemental analyzer. IR spectra in KBr (4500–500 cm⁻¹) were recorded using a Perkin-Elmer RXI FT-IR spectrophotometer. Electronic spectra in methanol (1200–200 nm) were recorded with a Hitachi U-3501 spectrophotometer. Electrochemical measurements were carried out using a computer-controlled PAR model 270 VERSASTAT electrochemical instrument with a glassy-carbon working electrode at SINP, Kolkata. All of the experiments were performed at 298 K with reference to the Ag/AgCl electrode of a solution of ca. 1 mM compound and 0.7 M Et₄NClO₄ in acetonitrile under an argon atmosphere.

Variable-temperature susceptibility measurements were carried out in the temperature range 2–300 K with an applied magnetic field of 0.1 T on polycrystalline samples of the three compounds with a Quantum Design MPMS-XL-5 SQUID magnetometer. The isothermal magnetizations were made at 2 K with magnetic fields of up to 5 T. The susceptibility data were corrected for the sample holder previously measured using the same conditions and for the diamagnetic contributions of the salt as deduced by using Pascal's constant tables ($\chi_{dia} = -184.1 \times 10^{-6}$, -172.7×10^{-6} , and -218.3×10^{-6} emu mol⁻¹ for 1–3, respectively).

Crystal Data Collection and Refinement. Single-crystal X-ray diffraction measurements for 1–3 were carried out on a Bruker Smart CCD-1000 diffractometer with Mo K α radiation ($\lambda = 0.71073$ Å) using both Φ - and ω -scan modes at 100 K. Intensity data were collected in a θ range of 1.97–27.52 for complex 1, 1.54–24.56 for complex 2, and 2.02–27.58 for complex 3.

Data reduction and cell refinements were performed with the SAINT program,⁹ and the absorption correction program SADABS¹⁰ was employed to correct the data for absorption effects. Crystal structures were solved by direct methods and refined with full-matrix least-squares (SHELXTL-97)¹¹ with atomic coordinates and anisotropic thermal parameters for all non-hydrogen atoms. The

crystal structure illustrations were generated using the Ortep-3¹² and Mercury programs. Significant crystallographic data are summarized in Table 1.

Results and Discussion

Synthesis. The reaction of the tridentate ligands HL¹, HL², and HL³ (Scheme 3) with a methanol solution of copper acetate monohydrate, triethylamine, and sodium nitrite yielded the respective nitrite complexes with general formula Cu(L^{*n*})(NO₂).

IR and Electronic Spectra. In the IR spectra, there are two sharp bands at 3306 and 3229 cm⁻¹ for complex 1 and 3306 and 3258 cm⁻¹ for complex 2, which are characteristic of the –NH₂ group in the Schiff base ligands. Complex 3 contains no significant peaks in the region of 3100 to 3300 cm⁻¹ since there is no NH₂ group. The bands corresponding to the azomethine (C=N) group occur at 1517, 1508, and 1508 cm⁻¹ for complexes 1, 2, and 3, respectively. In complex 1, the bands at 1337, 1169, and 837 cm⁻¹ are tentatively assigned to ν_s (NO₂), ν_{as} (NO₂), and δ (NO₂), respectively, as suggested recently for O-coordinated nitrite.¹³ The same bands are observed at 1370, 1069, and 828 cm⁻¹ and at 1365, 1029, and 830 cm⁻¹ for 2 and 3, respectively. The separation between the ν_{as} and ν_s bands corroborates the asymmetric chelating coordination of the nitrite ion.¹⁴

The electronic spectra of the three complexes display a single absorption band at 610, 608, and 587 nm in methanol, for complexes 1–3, respectively. The positions of these bands are consistent with the observed square-based geometry around the copper center.¹⁵ The intense band at about 375 nm for all three complexes is due to the ligand-to-metal charge transfer absorption bands due to nitrite.^{13,16} The bands

(11) Sheldrick, G. M. *SHELXTL 97*; University of Gottingen: Gottingen, Germany, 1997.

(12) Burnett, M. N.; Johnson, C. K. *ORTEP-3: Oak Ridge Thermal Ellipsoid Plot Program for Crystal Structure Illustrations, Report ORNL-6895*; Oak Ridge National Laboratory: Oak Ridge, TN, 1996.

(13) Lehnert, N.; Cornelissen, U.; Neese, F.; Ono, T.; Noguchi, Y.; Okamoto, K.; Fujisawa, K. *Inorg. Chem.* **2007**, *46*, 3916.

(14) Nakamoto, K. *Infrared and Raman Spectra of Inorganic and Coordination Compounds*, 4th ed.; Wiley: New York, 1986.

(15) Hathaway, B. J.; Tomlinson, A. A. G. *Coord. Chem. Rev.* **1970**, *5*, 1.

(16) Casella, L.; Carugo, O.; Gullotti, M.; Doldi, S.; Frassoni, M. *Inorg. Chem.* **1996**, *35*, 1101, and references therein.

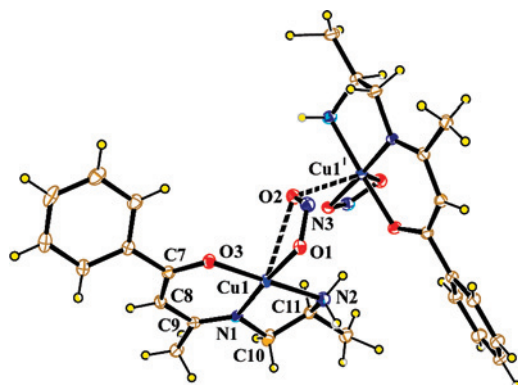
(9) SMART; SAINT, version 6.22a; Bruker AXS, Inc.: Madison, WI, 1999.

(10) Sheldrick, G. M. *SADABS*, version 2; University of Gottingen: Gottingen, Germany, 2001.

Table 2. Selected Bond Distances and Bond Angles^a

	1	2	3
Bond Distances			
Cu(1)–O(1)	2.011(2)	1.991(2)	1.984(2)
Cu(1)–O(2)	2.583(2)	2.703(2)	2.517(2)
Cu(1)–O(3)	1.909(2)	1.894(2)	1.912(2)
Cu(1)–N(1)	1.944(2)	1.936(2)	1.925(2)
Cu(1)–N(2)	1.995(2)	1.993(2)	2.044(2)
Cu(1)–O(2')	2.575(2)		
O(1)–N(3)	1.280(2)	1.281(3)	1.294(3)
O(2)–N(3)	1.246(2)	1.225(3)	1.239(3)
Bond Angles			
O(1)–Cu(1)–O(2)	53.07(6)	50.70(6)	54.84(7)
O(1)–Cu(1)–O(3)	87.50(7)	88.19(7)	89.48(7)
O(1)–Cu(1)–N(1)	176.36(8)	171.29(8)	169.78(8)
O(1)–Cu(1)–N(2)	93.24(8)	91.88(8)	93.29(7)
O(2)–Cu(1)–O(3)	89.46(6)	90.83(6)	85.97(7)
O(2)–Cu(1)–N(1)	129.98(6)	137.20(7)	115.64(8)
O(2)–Cu(1)–N(2)	89.37(7)	86.93(7)	105.61(7)
O(3)–Cu(1)–N(1)	94.38(8)	94.86(8)	93.62(8)
O(3)–Cu(1)–N(2)	177.84(7)	177.04(8)	167.44(7)
N(1)–Cu(1)–N(2)	84.99(8)	85.49(9)	85.78(8)
N(1)–Cu(1)–O(2')	93.87(7)		
N(2)–Cu(1)–O(2')	87.55(7)		
O(1)–Cu(1)–O(2')	82.86(6)		
O(2)–Cu(1)–O(2')	135.56(6)		
O(3)–Cu(1)–O(2')	94.56(7)		
O(1)–N(3)–O(2)	113.7(2)	114.7(2)	114.1(2)

^a Symmetry elements: $' = (3/2 - x, 1/2 + y, 1/2 - z)$ for complex **1** and $(1/2 + x, 3/2 - y, -z)$ for complex **2**.

**Figure 1.** ORTEP-3 view of complex **1** with ellipsoids at 30% probability.

at about 280 and 246 nm for all of the complexes may be attributed to the intraligand absorption band associated with $\pi \rightarrow \pi^*$ transition.¹⁶

Description of Crystal Structures. The basic building unit of these complexes (**1–3**) is $[\text{Cu}(\text{L}^n)(\text{NO}_2)]$, where L^n is the deprotonated monoanionic tridentate Schiff base ligand. This building unit is very similar in the three complexes, with some minor variations in bond distances or in bond angles (Table 2).

$[\text{Cu}(\text{L}^1)(\text{NO}_2)]_n$ (**1**). The molecular structure of **1** is shown in Figure 1 together with the common atom-numbering scheme. The most interesting feature of the structure of complex **1** is the formation of one-dimensional chains of $[\text{Cu}(\text{L}^1)(\text{NO}_2)]_n$ running parallel to the b axis (Figure S1, Supporting Information). The monomeric unit, $\text{Cu}(\text{L}^1)(\text{NO}_2)$, is constructed by one deprotonated monoanionic tridentate Schiff base ligand (L^1) and one $(\text{NO}_2)^-$ ion (Figure 1). The copper ion presents four short bonds, three with the ligand

L^1 through two nitrogen and one oxygen atom (N(1), N(2), and O(3)) and one with the nitrite ion via O(1) (all with bond lengths in the range 1.909(2)–2.011(2) Å, see Table 2). These four donor atoms form a deformed square-planar geometry with deviations from the mean coordination plane of $-0.046(2)$, $0.044(2)$, $0.045(2)$, and $-0.043(2)$ Å for N(1), N(2), O(3), and O(1), respectively, with the copper ion laying very close to this average plane. There is a weak interaction between the copper ion and the second oxygen O(2) of the coordinated nitrite at 2.583(2) Å, showing its unsymmetric chelating coordination mode. This semicoordinated¹⁷ oxygen is located in the axial position of a square pyramid. The opposite axial position (defining, thus, an elongated octahedral geometry) is occupied by another nitrite oxygen O(2') from a symmetry $(3/2 - x, 1/2 + y, 1/2 - z)$ -related unit at 2.575(2) Å, giving rise to the one-dimensional chain (Figures 1 and Supporting Information Figure S1).

It is worth mentioning that this bridging mode of nitrite in which the bridging oxygen atom, O(2), is far from both copper atoms, is very unusual. In fact, there is only one such reported example: $[\text{Cu}_2(\text{bdmap})(\text{NO}_2)_3(\text{H}_2\text{O})_4]$ (bdmap = 1,3-bis(dimethylamino)-2-propanolato(1-)).^{4b} Two other complexes having a similar bridging mode but with alternating “short–long” distances (Scheme 2c) have been reported in polynuclear $[\text{Cu}(\text{NO}_2)_2\text{CuL}]_n$ ($\text{L} = \text{N}, \text{N}'$ -bis(2-methyl-2-aminopropyl) oxamide)^{4a} and in dinuclear $[\text{Cu}_2\text{L}_2(\text{NO}_2)_2] \cdot \text{H}_2\text{O}$ ($\text{L} = 7$ -amino-4-methyl-5-aza-3-hepten-2-onato(1-)).⁶

Two of the carbon atoms (C11 and C13) of the Schiff base residue of complex **1** are disordered (occupancies of C11 and C13 are 0.75(1)). Therefore, we perform the conformational analysis with C11 and C13. The five-member chelate ring incorporating the dimethylene fragment from the starting diamine presents an envelope conformation on C(11) with puckering parameters $Q = 0.384(3)$ Å and $\phi = 288.8(3)^\circ$.¹⁸ However, the six-member chelate ring incorporating the benzoylacetone portion is nearly planar, with no atoms deviating from the least-squares plane by more than 0.026 Å.

In complex **1**, one of the amine hydrogen atoms, H(2a), of the Schiff base forms a hydrogen bond with the oxygen atom, O(3), of the tridentate Schiff base of the symmetrically related $(3/2 - x, 1/2 + y, 1/2 - z)$ unit, which is also connected by the nitrite bridge, Table 3 (Figure S1, Supporting Information). Thus, the one-dimensional chain structure of the compound is formed by both hydrogen and coordinate bonds. The complex shows no considerable π -stacking interaction between the aromatic rings. However, the molecules of one chain are stacked with those of another one via $\text{C}_{\text{sp}^3}\text{--H}\cdots\pi$ binding contacts to generate a two-dimensional network (Figure 2, Table 4). Each molecule of **1** interacts with symmetry-related $(1 - x, 2 - y, -z)$ neighboring molecules by means of weak $\text{C}_{\text{sp}^3}\text{--H}\cdots\pi$ (phenyl) supramolecular interactions (the distance $\text{H1}\cdots\text{centroid A}$ is 3.20(1) Å, the angle $\text{C13--H1}\cdots\text{C}_g$ (ring A) is $145.1(1)^\circ$,

(17) Palopoli, S. F.; Geib, S. J.; Rheingold, A. L.; Brill, T. B. *Inorg. Chem.* **1988**, *27*, 2963, and references therein.

(18) (a) Cremer, D.; Pople, J. A. *J. Am. Chem. Soc.* **1975**, *97*, 1354. (b) Boyens, J. C. A. *J. Cryst. Mol. Struct.* **1978**, *8*, 31.

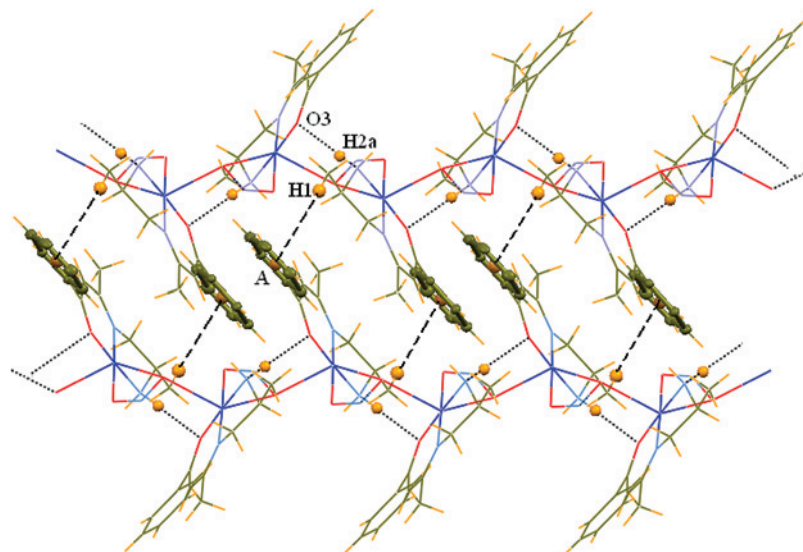


Figure 2. Extended hydrogen-bonding network along with the CH- π ring interaction in the supramolecular unit of complex **1**.

Table 3. Hydrogen Bonding Distances (Å) and Angles (deg) for Complexes **1** and **2**

Complex	D-H...A	D-H	D...A	A...H	\angle D-H...A
1	N2-H2a...O3 ^a	0.899	3.011(2)	2.118	171.8(2)
2	N2-H2a...O2 ^b	0.810	3.058(3)	2.260	170.0(2)
	N2-H2b...O1 ^c	0.820	2.959(3)	2.330	134.0(3)

^a $3/2 - x, 1/2 + y, 1/2 - z$. ^b $-x, 2 - y, -z$. ^c $1/2 + x, 3/2 - y, -z$.

and the distance C13...C_g (ring A) is 4.03(1) Å. This C_{sp}³-H... π contact distance is typical for this type of interaction.¹⁹

[Cu(L²)(NO₂)] (2) and [Cu(L³)(NO₂)] (3). The structures of complexes **2** and **3** are shown in Figure S2 (Supporting Information) and Figure 3, respectively, with the common atom numbering scheme. Selected bond lengths and angles of these complexes are given in Table 2. For both complexes, the structures consist of Cu(Lⁿ)(NO₂) units. As in **1**, three donor atoms, N(1), N(2), and O(3), of the ligand L² or L³ and one oxygen atom O(1) of the nitrite ligand form the equatorial plane in complexes **2** and **3**. Deviations of donor atoms N(1), N(2), O(3), and O(1) from their mean plane are -0.097(2), 0.096(2), 0.095(2), and -0.094(2) Å, respectively, for **2** and -0.198(2), 0.189(2), 0.195(2), and -0.186(2) Å, respectively, for **3**. The central Cu(II) atom is located nearly on the mean plane (with deviations of only 0.007(1) and 0.003(1) Å in complexes **2** and **3**, respectively). In both complexes, the mean Cu-N distances (1.965 and 1.984 Å for **2** and **3**, respectively) are, as expected, slightly longer than those of Cu-O ones (1.942 and 1.948 Å for **2** and **3**, respectively). The five-member chelate ring incorporating the dimethylene fragment from the diamine shows an envelope conformation on C(11) in both complexes ($Q = 0.400(2)$ Å, $\phi = 99.2(3)^\circ$ for complex **2** and $Q = 0.419(2)$ Å and $\phi = 294.7(3)^\circ$ for complex **3**).¹⁸ In complex **3**, the six-member chelate ring incorporating the benzoylacetone residue has a

conformation intermediate between envelope and screw-boat conformations,¹⁸ with $Q = 0.254(2)$ Å, $\theta = 116.7(5)^\circ$, and $\phi = 186.9(6)^\circ$. On the contrary, in complex **2**, this chelating ring is quite planar, with maximum deviations from the least-squares plane of less than 0.021 Å, indicating a better delocalization of the electron cloud²⁰ compared to that of complex **3**. Besides the four short Cu-N and Cu-O bond distances, in both complexes, there is a long Cu-O bond formed by the other O atom of the nitrite ligand, O(2), with bond distances of 2.703(2) and 2.517(2) Å in complexes **2** (Figure S2, Supporting Information) and **3** (Figure 3), respectively. This long Cu...O(2) bond renders the coordination geometry around the Cu(II) ion into a square pyramid. In this context, it may be mentioned that, in several other Cu(II) nitrite complexes, similar long Cu-O distances were considered as semicoordination.¹⁷ Moreover, the Cu(1)-O(1)-N(3) angles of the complexes **1-3** (110.1(2)°, 114.2(2)°, and 107.4(2)° for complexes **1, 2**, and **3**, respectively), which are intermediate between 119.5° for monodentate and 93-100° for symmetric bidentate coordination modes, are in good agreement with the asymmetric chelating coordination of nitrite to Cu(II).²¹ In complex **2**, in the other axial position of Cu(II), there is also a very weak intermolecular Cu...N contact (2.956 Å), but the distance is too long to be considered a bond.

In complex **2**, both amine hydrogen atoms of the Schiff base ligand form hydrogen bonds with the oxygen atoms of the nitrite ion of neighboring units. Thus, H(2a) is linked with O(2') ($' = 1/2 + x, 3/2 - y, -z$) of the nitrite group (Figure 4, Table 3), and O(2) is linked with H(2a') of the same unit to form a hydrogen-bonded dimer. Furthermore, H(2b) forms a hydrogen bond with the equatorially coordi-

(19) (a) Lu, Z.; Gamez, P.; Mutikainen, I.; Turpeinen, U.; Reedijk, J. *Cryst. Growth Des.* **2007**, *7*, 1669. (b) Nishio, M. *Cryst. Eng. Comm.* **2004**, *6*, 130, and references therein.

(20) Sarkar, B.; Bocelli, G.; Cantoni, A.; Ghosh, A. *Polyhedron* **2008**, *27*, 693, and references therein.

(21) (a) Youngme, S.; Chaichit, N.; Koonsaeng, N. *Inorg. Chim. Acta* **2002**, *335*, 36. (b) Youngme, S.; Chaichit, N.; Pakawatchai, C.; Booncoon, S. *Polyhedron* **2002**, *21*, 1279, and references therein. (c) Komeda, N.; Nagao, H.; Kushi, Y.; Adachi, G.; Suzuki, M.; Uehara, A.; Tanaka, K. *Bull. Chem. Soc. Jpn.* **1995**, *68*, 581.

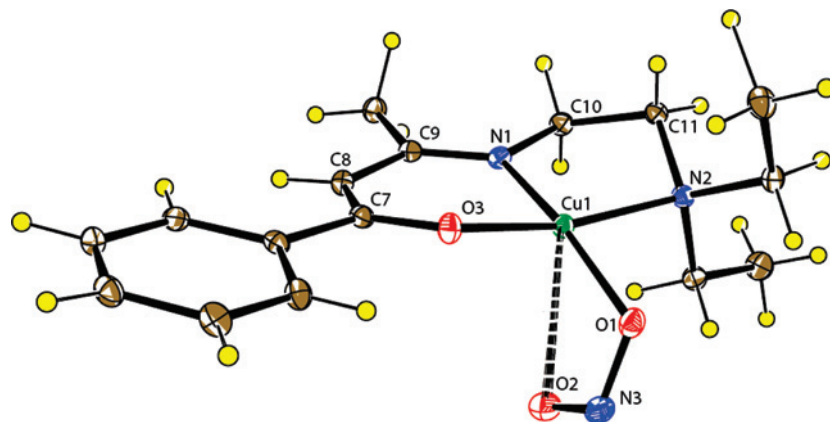


Figure 3. ORTEP-3 view of complex **3** with ellipsoids at 30% probability.

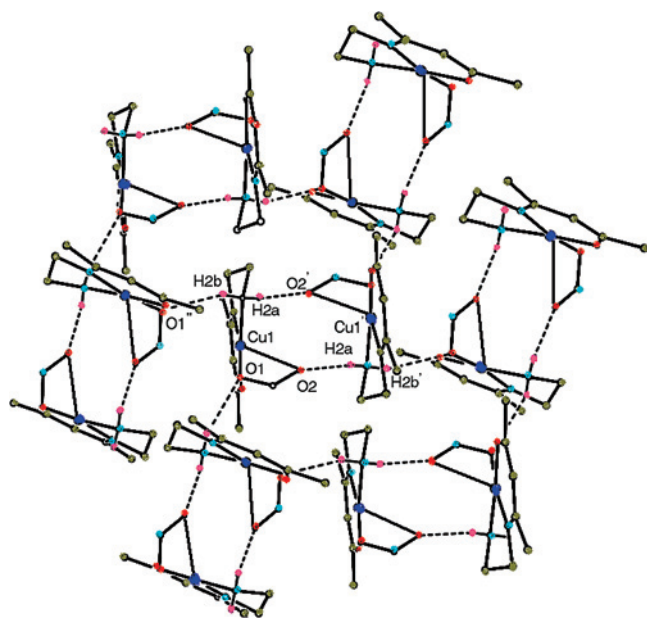


Figure 4. Extended hydrogen-bonded network of complex **2**. Symmetry transformations: $' = 1/2 + x, 3/2 - y, -z$; $'' = 1/2 - x, y, -1/2 + z$.

nated oxygen atom, O(1'') ($'' = -x, 2 - y, -z$) of the neighboring dimers to form a hydrogen-bonded network (Figure 4). Complex **3** does not show any hydrogen bond.

As with complex **1**, complexes **2** and **3** do not show any considerable π -stacking interaction between the aromatic rings, but they show $C_{sp^2}-H\cdots\pi$ and $C_{sp^3}-H\cdots\pi$ stacking interactions, giving rise to two-dimensional networks (Figure S3, Supporting Information, and Figure 5, respectively for complexes **2** and **3**). Each molecule of **2** interacts with symmetry-related $(1/2 - x, 1/2 + y, z)$ neighboring molecules by means of weak $C_{sp^3}-H\cdots\pi$ (phenyl) supramolecular interactions (with an H6 \cdots centroid A distance of 2.77(1) Å, a C12–H6 $\cdots\pi(C_g)$ (ring A) angle of 149.67(2) $^\circ$, and a C12 $\cdots\pi(C_g)$ (ring A) distance of 3.65(1) Å). Furthermore, each

molecule of **2** also interacts with symmetry-related $(1 + x, y, z)$ neighboring molecules by means of $C_{sp^2}-H\cdots\pi$ (phenyl) supramolecular interactions (with an H4 \cdots centroid A distance of 2.81(1) Å, a C10–H4 $\cdots\pi(C_g)$ (ring A) angle of 139.84(1) $^\circ$, and a C10 $\cdots\pi(C_g)$ (ring A) distance of 3.61(1) Å). These $C_{sp^2}-H\cdots\pi$ contact parameters are typical for this type of interaction.¹⁹ Supporting Information Figure S3 (Table 4) illustrates the supramolecular interaction in complex **2**. Complex **3** shows similar $C_{sp^2}-H\cdots\pi$ and $C_{sp^3}-H\cdots\pi$ stacking interactions, as illustrated in Figure 5 (Table 4).

Electrochemistry. All three complexes (**1**, **2**, and **3**) in acetonitrile solution display reductive responses attributed to the Cu(II)/Cu(I) couple (E_p) at -0.97 , -0.83 , and -0.69 V, respectively, whereas the corresponding oxidative responses for the Cu(I)/Cu(II) couple (E_p) are observed at -0.78 , -0.65 , and -0.51 V for complexes **1**, **2**, and **3** respectively (Figure 6), during the anodic potential scan. The potential values are within the range of other Cu(II)–Schiff-base complexes.²² In complexes **1** and **2**, a second oxidative response is observed in the anodic potential scan at ca. -0.21 V with a very narrow width and high peak current. This response is typical of the anodic stripping of copper.^{22d,23} Therefore, it may be assumed that, on the electrode surface, Cu(II) complexes **1** and **2** are reduced to Cu(I), and these are not stable and undergo disproportionation to Cu⁰ and Cu²⁺. The considerably low values of i_{pa}/i_{pc} of **1** and **2** (for example 0.64 and 0.73, respectively, at scan rate 400 mV s⁻¹) corroborate the disproportionation. It is worth mentioning that this anodic stripping is more pronounced at lower scan rates (50 or 100 mV s⁻¹), and at very high scan rates (1000 mV s⁻¹) this peak almost disappears for both complexes. The relative current height of the Cu(I)/Cu(II) oxidative response, that is, the i_{pa}/i_{pc} ratio, increases with the scan rate. Thus, the longer the time that the Cu(I) species

Table 4. CH- π Supramolecular Interaction Bonding Distances (Å) and Angles (deg) for Complexes **1**, **2**, and **3**

complex	$C_{sp^2}/C_{sp^3}-H\cdots\pi(C_g)$	$H\cdots\pi(C_g)$ (Å)	$X\cdots\pi(C_g)$ (Å)	$C_{sp^2}/C_{sp^3}-H\cdots\pi(C_g)$ (deg)
1	C13–H1 $\cdots\pi(C_g)$ 4)	3.205	4.030	145.07
2	C10–H4 $\cdots\pi(C_g)$ 3)	2.811	3.610	139.84
	C12–H6 $\cdots\pi(C_g)$ 3)	2.777	3.653	149.67
3	C12–H10 $\cdots\pi(C_g)$ 4)	3.042	3.693	131.92
	C13–H23 $\cdots\pi(C_g)$ 4)	2.749	3.683	158.38

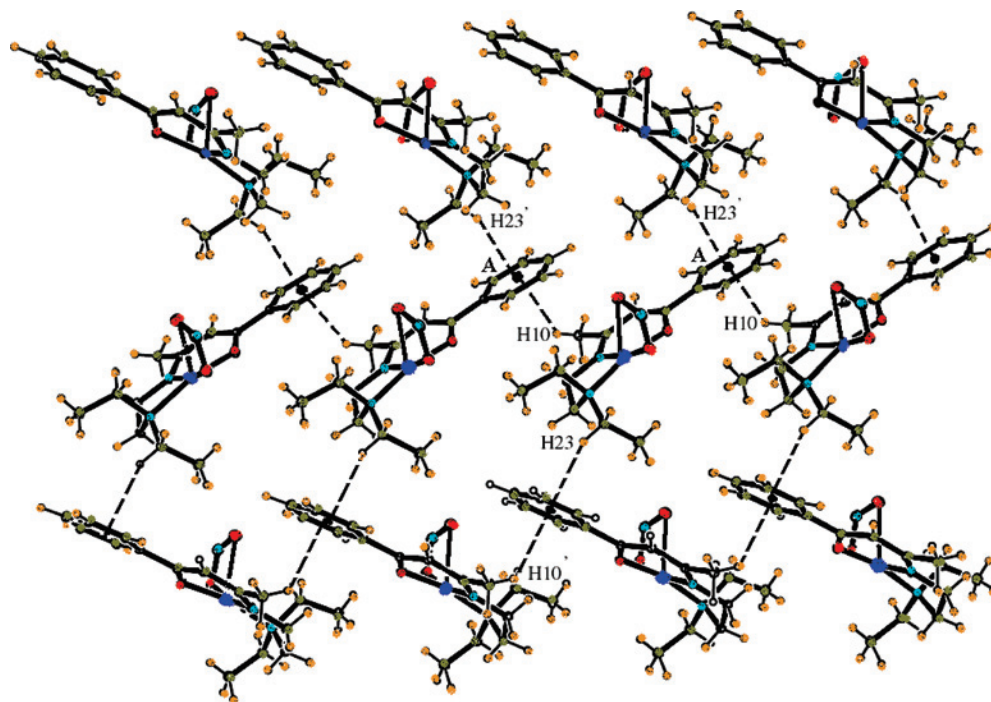


Figure 5. CH- π ring interaction in the supramolecular unit of complex **3**.

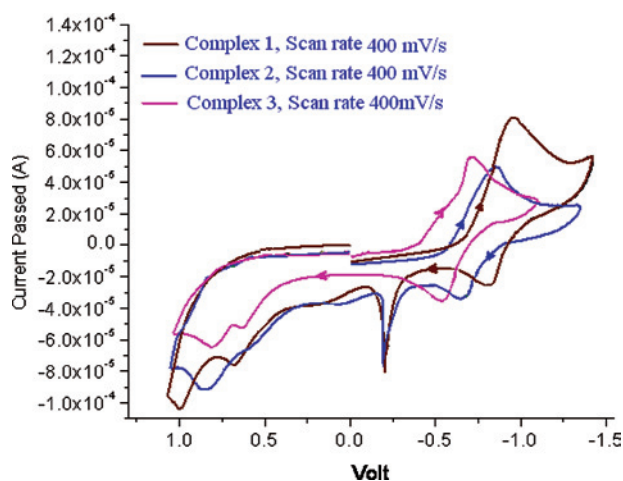


Figure 6. The cyclic voltammogram of complexes **1**, **2**, and **3** in acetonitrile solution.

remains on the electrode surface is, the higher the disproportionation of Cu(I) to Cu⁰ and Cu²⁺ is. In complex **3**, no anodic stripping is observed, even at a low scan rate of 50 mV s⁻¹, indicating the stability of the Cu(I) species. Such anodic stripping has also been found in a few other Cu(II)–Schiff-base complexes.^{22d,23} In all three complexes, the axial bonds are rather weak, and it is not clear if the same structures that have been determined by crystallography exist also in acetonitrile solution. Therefore, it is difficult to correlate the reduction potentials or the stabilities of reduced species with the solid-state structures of the complexes, especially with the polynuclear structure of **1**. However, the anodic shift of the potential values of complexes **1–3** as well as the stability of the +1 oxidation state in complex **3** may be explained in terms of tetrahedral distortion of the equatorial coordination plane around the copper atom. It is well known that higher tetrahedral distortion stabilizes the

+1 oxidation state of copper.^{20,24} The tetrahedral distortion is calculated by the dihedral angles between the two planes formed by the N(1), Cu, and O(3) atoms and the N(2), Cu, and O(1) atoms, and these are found to be 3.65°, 8.60°, and 15.50° for complexes **1**, **2**, and **3**, respectively (compared with 0° for a square-planar geometry and 90° for a perfect tetrahedron). In all of the complexes, the appearance of an irreversible anodic response at a comparatively high applied voltage (~ 0.96 V) may be attributed to the oxidation of the nitrite group, as reported earlier.²⁵

Magnetic Properties. The thermal variation of the product of the molar magnetic susceptibility times the temperature ($\chi_m T$) per Cu(II) ion for complex **1** shows a room-temperature value of 0.43 emu K mol⁻¹, close to the expected value for isolated Cu(II) ions with an $S = 1/2$ spin ground state (0.375 emu K mol⁻¹). When the sample is cooled, $\chi_m T$ shows a smooth linear decrease down to ca. 100 K, and below this temperature, it shows a more pronounced decrease to reach a value of ca. 0.18 emu K mol⁻¹ at 2 K (Figure 7). This behavior indicates that complex **1** presents antiferromagnetic exchange interactions between the Cu(II) ions. Although the structure of complex **1** shows quasi-isolated Cu(II) ions, there are short intermolecular contacts through the terminal oxygen atom of the nitrite ligand and the Cu(II) ion of the

(22) (a) Lintvedt, R. L.; Kramer, L. S. *Inorg. Chem.* **1983**, *22*, 796. (b) Mukherjee, A.; Rudra, I.; Naik, S. G.; Ramasesha, S.; Nethaji, M.; Chakravarty, A. R. *Inorg. Chem.* **2003**, *42*, 5660. (c) Lintvedt, R. L.; Ranger, G.; Schoenfelner, B. A. *Inorg. Chem.* **1984**, *23*, 688. (d) Robandt, P. V.; Schroeder, R. R.; Rorabacher, D. B. *Inorg. Chem.* **1993**, *32*, 3957.

(23) (a) Ray, U.; Banerjee, D.; Mostafa, G.; Lu, T. H.; Sinha, C. R. *New J. Chem.* **2004**, *28*, 1437. (b) Santra, B. K.; Reddy, P. A. N.; Nethaji, M.; Chakravarty, A. R. *Inorg. Chem.* **2002**, *41*, 1328.

(24) Itoh, S.; Kishikawa, N.; Suzuki, T.; Takagi, H. D. *Dalton Trans.* **2005**, 1066, and references therein.

(25) Scarpellini, M.; Neves, A.; Castellano, E. E.; Neves, E. F. A.; Franco, D. W. *Polyhedron* **2004**, *23*, 511, and references therein.

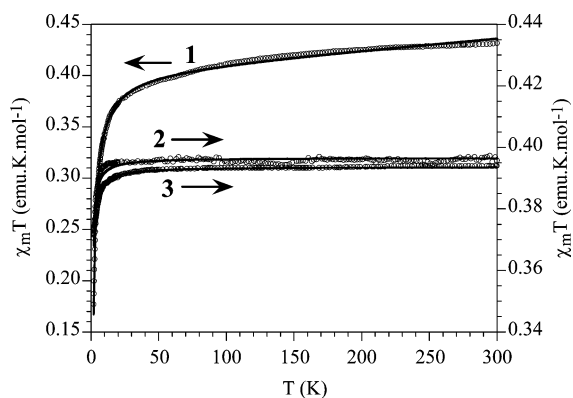


Figure 7. Thermal variation of the $\chi_m T$ product of compounds **1–3**. Solid lines are the best fits to the models (see text).

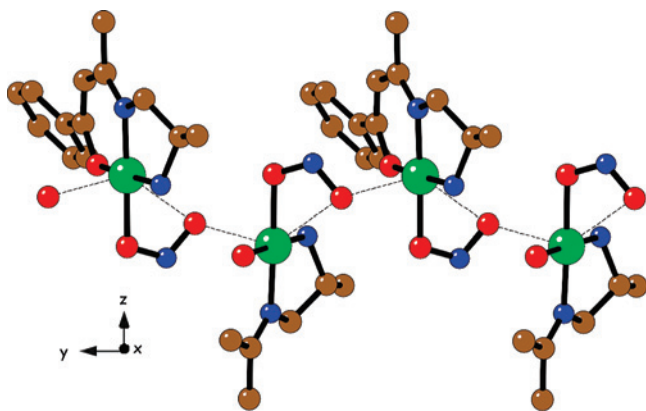


Figure 8. View of the $-\text{Cu}-\text{ONO}-\text{Cu}-$ chains along the b axis in compound **1**. Dotted lines represent the shortest $\text{Cu}-\text{O}$ intermolecular contacts.

neighboring molecule, with a $\text{Cu}-\text{O}$ distance of 2.575 Å. Thus, complex **1** can be better described from the magnetic point of view as a $\text{Cu}(\text{II})$ regular chain with $\text{Cu}-\text{ONO}\cdots\text{Cu}$ bridges (Figure 8). Accordingly, we have fitted the magnetic properties of complex **1** to the model proposed by Hatfield et al.²⁶ for an $S = 1/2$ regular antiferromagnetic chain plus a temperature-independent paramagnetism ($N\alpha$) to account for the linear decrease of $\chi_m T$ at high temperatures. This model reproduces very satisfactorily the magnetic data in the whole temperature range with the following set of parameters: $g = 2.081(1)$, $J = -1.96(2) \text{ cm}^{-1}$ (the Hamiltonian is written as $H = -JS_i S_j$), and $N\alpha = 109(2) \times 10^{-6} \text{ emu mol}^{-1}$ (solid line in Figure 7).

The $\chi_m T$ products for complexes **2** and **3** are very similar, as expected from the similarities observed in their structures (see above). Thus, both compounds show a room-temperature value of ca. 0.40 emu K mol^{-1} , close to that of compound **1** and also to the expected value for an $S = 1/2$ spin ground state with $g = 2$. When cooling down the sample, $\chi_m T$ remains constant down to ca. 10 K for both complexes, and below this temperature, a faint progressive decrease is seen in both compounds, to reach values of ca. 0.37 and ca. 0.38 emu K mol^{-1} at 2 K (Figure 7) in complexes **2** and **3**, respectively. This behavior indicates that complexes **2** and

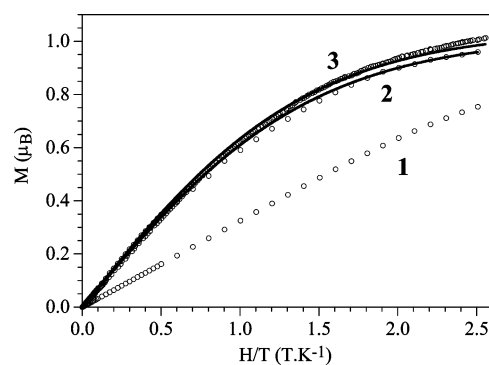


Figure 9. Isothermal magnetization of compounds **1–3** at 2 K. Solid line represents the best fit to the Brillouin function (see text).

3 are essentially paramagnetic with very weak antiferromagnetic couplings, as indicated by the slight decrease at low temperatures. Since the structures of these two compounds show that the complexes do not present any important covalent bonds between the mononuclear units, we can conclude that the weak antiferromagnetic coupling must arise from the weak intermolecular interactions (hydrogen bonds in compound **2** and $\text{C}_{\text{sp}^2}-\text{H}\cdots\pi$ and $\text{C}_{\text{sp}^3}-\text{H}\cdots\pi$ stacking interactions in **2** and **3**) observed in these complexes (see above). Since these weak intermolecular interactions connect each complex with its four nearest neighbors, generating a 2D network (Figures 4 and 5), we have fitted the magnetic properties of both compounds with the quadratic layer antiferromagnetic model of Lines.²⁷ This model reproduces very satisfactorily the magnetic data of complexes **2** and **3** (solid line in Figure 7) with the following parameters: $g = 2.0583(2)$ and $J = -0.089(2) \text{ cm}^{-1}$ for compound **2** and $g = 2.0490(2)$ and $J = -0.096(1) \text{ cm}^{-1}$ for compound **3** (the Hamiltonian is written as $H = -JS_i S_j$). As expected from the weak intermolecular contacts, the magnetic coupling in both complexes is almost negligible and significantly smaller than that in compound **1**.

The isothermal magnetization of complex **1** at 2 K shows an almost linear behavior without reaching saturation up to 5 T, where the value is ca. 0.7 μ_B , below the expected value of 1.0 μ_B for a paramagnetic $S = 1/2$ system (Figure 9). This behavior confirms the antiferromagnetic coupling shown by this compound. Thus, any attempt to fit this behavior with a Brillouin function leads to a very low g value and a very poor fit. Complexes **2** and **3** show very similar magnetization plots with a saturation slightly above 1.0 μ_B , which is the expected value for an isolated $S = 1/2$ $\text{Cu}(\text{II})$ ion, in agreement with the absence of exchange interactions. This absence of significant interactions is confirmed by the fact that the isothermal magnetizations in complexes **2** and **3** can be well reproduced with a Brillouin function with $S = 1/2$ and g values of 2.045(5) and 2.090(2) (solid line in Figure 9).

The antiferromagnetic exchange coupling found in complex **1** can be rationalized on the basis of three structural facts: (i) The NO_2 ligand connects an axial position of one $\text{Cu}(\text{II})$ ion with an equatorial position of the neighboring one.

(26) Brown, D. B.; Donner, J. A.; Hall, J. W.; Wilson, S. R.; Wilson, R. B.; Hodgson, D. J.; Hatfield, W. E. *Inorg. Chem.* **1979**, *18*, 2635.

(27) Lines, M. E. *J. Phys. Chem. Solids* **1970**, *31*, 101.

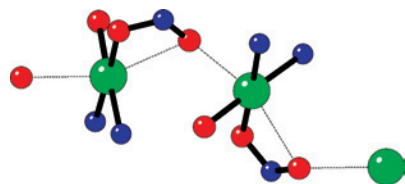


Figure 10. Coordination environment of the Cu(II) ions in compound **1**. Dotted lines are the long Cu...O contacts.

This situation leads to a poor overlap of the $d_{x^2-y^2}$ magnetic orbitals of both Cu(II) ions. (ii) The long Cu...O axial distance (2.575 Å) also reduces the overlap of the Cu(II) magnetic orbital with the orbitals of the nitrito ligand. (iii) The dihedral angles formed by the $\mu_{1,3}$ -NO₂ bridge and the equatorial planes of the two Cu(II) ions connected are 91.3° (NO₂ in equatorial position) and 37.4° (NO₂ in axial position), also precluding a good overlap of the orbitals (Figure 10). As far as we know, there is only one reported example of a $\mu_{1,3}$ -NO₂ bridged Cu(II) complex: [Cu(pyrazine)₂NO₂](ClO₄).^{2b} This compound presents symmetric $\mu_{1,3}$ -NO₂ bridges whose magnetic coupling is considered negligible compared with that through the pyrazine bridges (which is also weak and antiferromagnetic). Since complex **1** is the only known asymmetric $\mu_{1,3}$ -NO₂ bridged complex, it is not possible to establish any magneto-structural correlation. Nevertheless, we can estimate that the coupling through an asymmetric $\mu_{1,3}$ -NO₂ bridge connecting axial positions of the Cu(II) ions must be weak and antiferromagnetic, in agreement with the experimental result.

The very weak (although not zero) magnetic exchange observed in complexes **2** and **3** is in agreement with the expected results and indicates very weak intermolecular interactions (hydrogen bonds in compound **2** and C_{sp²}-H... π and C_{sp³}-H... π stacking interactions in **2** and **3**). Finally, a last possible pathway might include the dipolar interactions that may also contribute to the antiferromagnetic exchange. Nevertheless, given the long Cu-Cu distances, these dipolar interactions seem to be almost negligible.

Conclusions

The syntheses and crystal structures of three new complexes of Cu(II) nitrite with 1-benzoylacetone-derived N,N,O donor Schiff base ligands show that a slight variation in the coligands can bring about a subtle change in the coordination mode of the nitrite ion. As a consequence, the resulting molecule may have a very different structural topology. The one-dimensional chain structure of compound **1**, formed by a rare type of μ -nitrito-1 κ^2 O, O' :2 κ O tridentate bridging mode of the nitrite, shows the presence of weak, but noticeable, antiferromagnetic exchange interactions. Magnetic measurements of **2** and **3** reveal that the compounds are essentially paramagnetic, with very weak antiferromagnetic couplings, which are attributed to the intermolecular H-bonding and C_{sp²}-H... π and C_{sp³}-H... π stacking interactions. The electrochemical study of the complexes shows that the reduced Cu(I) species of complexes **1** and **2** are unstable and undergo disproportionation on the time scale of electrochemical experiments. The anodic shift of the reduction potential and the resistance to the disproportionation of the derived Cu(I) species of **3** may be attributed to the higher tetrahedral distortion in the equatorial plane of the complex.

Acknowledgment. The authors thank Prof. P.C. Mondal and Mr. P.S. Guin, Saha Institute of Nuclear Physics, Kolkata, for assistance in the recording and interpretation of CV data. The authors acknowledge the European Union for financial support (MAGMANet network of excellence) and the Spanish Ministerio de Educación y Ciencia (Projects MAT2007-61584 and Consolider-Ingenio 2010 CSD 2007-00010 in Molecular Nanoscience).

Supporting Information Available: Crystallographic data in CIF format for the structures reported; additional figures. This material is available free of charge via the Internet at <http://pubs.acs.org>.

IC8011519